

# Geometrical analysis of optical transmission characteristics of prism sheet layers

Hwi Kim  
Yong Jun Lim  
Byungchoon Yang  
Kyongsik Choi  
Byounggho Lee, FELLOW SPIE  
Seoul National University  
School of Electrical Engineering  
Kwanak-Gu Shinlim-Dong  
Seoul 151-744, Korea  
E-mail: byounggho@snu.ac.kr

**Abstract.** We analyze the optical transmission characteristics of prism sheet layers based on a geometrical approach. An analytic method for finding the radiant intensity profile of the light transmitted through a single prism sheet for an incident light with arbitrary radiant intensity profile is developed. It is shown that the output radiant intensity profile is the inner product of the newly defined partial transmission coefficient distribution of the prism sheet and the input radiant intensity profile. The developed analysis method for a single prism sheet is immediately generalized to analyze prism sheet layer being composed of several prism sheets.

© 2005 Society of Photo-Optical Instrumentation Engineers. [DOI: 10.1117/1.2148450]

Subject terms: prism sheet; prism sheet layer; geometrical analysis; transmission characteristics; radiant intensity.

Paper 040903R received Nov. 30, 2004; revised manuscript received Apr. 22, 2005; accepted for publication May 6, 2005; published online Jan. 4, 2006.

## 1 Introduction

A prism sheet is an essential element for the backlight modules of thin-film-transistor liquid crystal displays (TFT-LCDs), which enhances the luminance and viewing angle of TFT-LCDs. Many patents are already held for prism sheets and backlight modules.<sup>1-5</sup> Now, among these, 3M brightness enhancement films (BEFs) are perceived<sup>1-3</sup> to be the de facto standard, although they have a simple geometric structure. In the industrial world, it is commonly understood that a new prism sheet design that is competitive with a BEF and simultaneously not touched by 3M's patents is challenging.

BEF is the simplest prism sheet that is a periodic array of elementary prisms and is characterized by just three design parameters, the refractive index of material and two base angles. Hence, the transmissivity of the BEF is a function of these three parameters. Coincidentally, even using a commercial ray-trace simulator is somewhat cumbersome for studying the structural relationship among the transmissivity and the design parameters, since laborious repetition of simulation with a consecutive change of each parameter requires heavy computation time. Moreover, such repeated simulations do not provide a clear description of the relationship among the transmissivity and the design parameters.

In general, however, prism sheets including BEF are inevitably analyzed and designed using commercial ray-trace simulators, since the full behavior of light inside prism sheets is too complex to be modeled definitely. Multiple internal reflections inside prism sheets and multiple scattering between adjacent prisms on prism sheets increase the complexity. Although the trace of a ray through prism sheet can be exactly simulated using simple geometrical rules, a collective behavior of numbers of rays is difficult to under-

stand. Such a ray tracing requires a long computation time, which is a practical bottleneck in the design work.

Therefore, for the design task, intuitive and fast algorithms for analyzing a target structure are required. In this paper, an analytic approach to understand the collective behavior of ray bundles (light) is developed under the first order approximation. The first order approximation means ignoring multiple internal reflections and scatterings. The objective of this paper is to provide an intuitive and fast analytic algorithm that would be useful for devising new ingenious designs of prism sheets.

This paper is organized into three sections. In Sec. 2, a geometrical analysis on the transmissivity of a single prism sheet is developed. In Sec. 3, the analysis method is generalized to be applicable to prism sheet layers. Final remarks are addressed in Sec. 4.

## 2 Geometrical Analysis on the Transmissivity of a Single Prism Sheet

In this paper, it is assumed that the light source illuminating prism sheets is incoherent and can be completely characterized by the radiant intensity profile.<sup>6,7</sup> Thus, the total response of the prism sheet for the light source is equivalently represented by an incoherent superposition of independent responses of prism sheets of each plane wave component of the radiant intensity profile. Therefore, the first step of the analysis is to account for the transmissivity of a prism sheet for an obliquely incident plane wave.

Under the first-order approximation, the proposed method does not take multiple reflections inside prism sheet and multiple scattering between adjacent unit prisms into account. Hence, considering the periodicity of the prism sheet, we can see that investigating just one unit prism of the prism sheet is enough to account for the full behavior of the prism sheet. Theoretically, if the Fresnel's transmission coefficients are relatively bigger than the reflection coefficients in the ray tracing, that is, the refractive index is relatively low, the portion of the energy allocated in the mul-

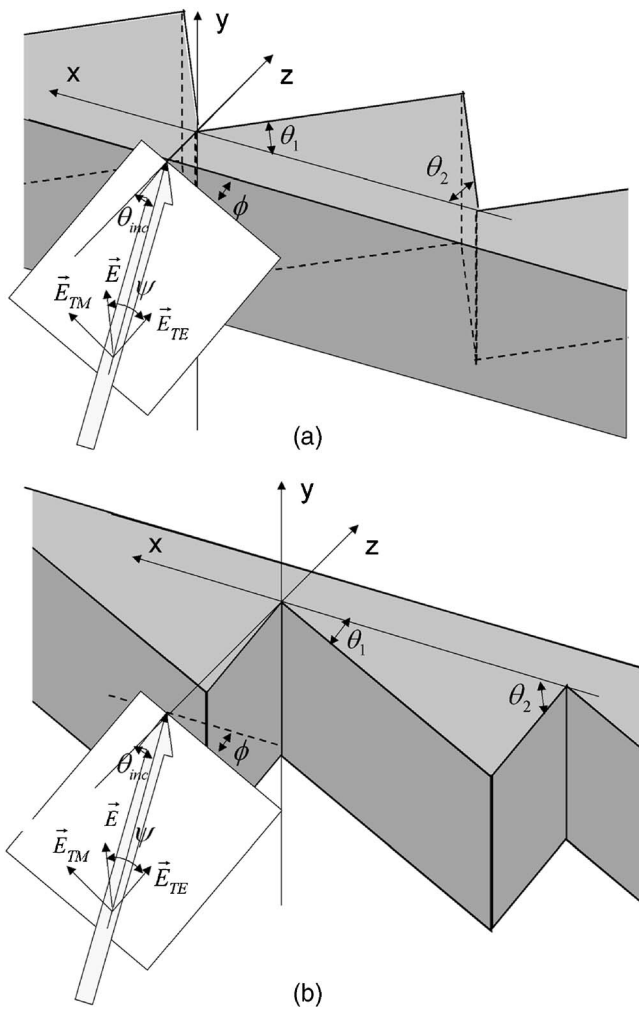


**Fig. 1** Incident plane wave with incidence angle of  $\theta_{inc}$ , azimuthal angle of  $\phi$ , and polarization angle of  $\psi$  incident on (a) the rear side and (b) the front side of a prism sheet.

multiple internal reflections and the scattering may be small relative to the portion of the first-order transmitted and reflected power.

Intuitively, we can see that there are two cases of the illumination of a plane wave on a prism sheet: the rear side or the front side of prism sheets may be illuminated. On the other hand, the classification of the two cases is due to the mathematical convenience. Mathematically, the details of the calculation procedure of the two cases are considerably different. Thus, two cases are separately analyzed and compared. In this section, the transmissivity of a prism sheet for an obliquely incident plane wave is analyzed based on geometrical optical approach, which is called local plane wave method.<sup>8</sup> Figure 1 shows that an incident plane wave with an incidence angle of  $\theta_{inc}$ , an azimuthal angle of  $\phi$ , and a polarization angle of  $\psi$  is respectively incident on the rear side and the front side of a prism sheet. It is assumed that the prism sheet is a periodic array of an elementary prism with refractive index of  $n$ , and base angles  $\theta_1$  and  $\theta_2$ , as indicated in Fig. 1.

In the first and second subsections, the cases of the incidence on the rear side and the front side of prism sheets

are investigated, respectively. In the third subsection, the analysis method of optical transmission characteristics of a single prism sheet for general light sources with arbitrary radiant intensity profile is addressed.

## 2.1 Oblique Incidence of a Plane Wave on the Rear Side of Prism Sheets

The transmissivity of the prism sheet is considered when an incident plane wave propagates from the rear side to the front side of a prism sheet with simple geometric approach [see Fig. 1(a)]. In this paper, since only the intensity and the direction of the local plane wave are a matter of concern, constant phase variation induced by the propagation of a local plane wave along a finite distance is ignored. Figure 2 shows traces of rays passing through facets of the prism sheets. We separately look into ray trace along two separated paths,  $S_1^A \rightarrow S_2^A$  and  $S_1^B \rightarrow S_2^B$ , respectively, indicated in Fig. 2(a).

At first, the intensity of the optical wave transmitted through each path in the prism sheet should be obtained. Let the electric field in the region I be denoted by  $\mathbf{E}_1$ . Then, it is represented as

$$\mathbf{E}_1 = (u_{1,x}\hat{x} + u_{1,y}\hat{y} + u_{1,z}\hat{z})\exp[j(k_{1,x}x + k_{1,y}y + k_{1,z}z)], \quad (1a)$$

where  $(u_{1,x}, u_{1,y}, u_{1,z})$  and  $(k_{1,x}, k_{1,y}, k_{1,z})$  are, respectively, defined as

$$\begin{aligned} (u_{1,x}, u_{1,y}, u_{1,z}) = & E_0(\cos\psi \cos\theta_{inc} \cos\phi \\ & - \sin\psi \sin\phi, \cos\psi \cos\theta_{inc} \sin\phi \\ & + \sin\psi \cos\phi, -\cos\psi \sin\theta_{inc}), \end{aligned} \quad (1b)$$

and

$$\begin{aligned} (k_{1,x}, k_{1,y}, k_{1,z}) = & (k_0 \sin\theta_{inc} \cos\phi, k_0 \sin\theta_{inc} \sin\phi, \\ & k_0 \cos\theta_{inc}), \end{aligned} \quad (1c)$$

where the incidence angle  $\theta_{inc}$  is in the range of  $0 \leq \theta_{inc} < 90$  deg. When  $\mathbf{E}_1$  meets the bottom facet of the prism sheet,  $\mathbf{E}_1$  is refracted into the prism sheet [denoted by region II in Figs. 2(b) and 2(c)]. Let the refracted wave in the region II denoted by  $\mathbf{E}_2$ . Then, it is represented as

$$\mathbf{E}_2 = (u_{2,x}\hat{x} + u_{2,y}\hat{y} + u_{2,z}\hat{z})\exp[j(k_{2,x}x + k_{2,y}y + k_{2,z}z)], \quad (2a)$$

where  $(u_{2,x}, u_{2,y}, u_{2,z})$  and  $(k_{2,x}, k_{2,y}, k_{2,z})$  are, respectively, defined as

$$(u_{2,x}, u_{2,y}, u_{2,z}) = (\tau_x^A u_{1,x}, \tau_y^A u_{1,y}, \tau_z^A u_{1,z}), \quad (2b)$$

and

$$(k_{2,x}, k_{2,y}, k_{2,z}) = \{k_{1,x}, k_{1,y}, k_0 n [1 - (\sin\theta_{inc}/n)^2]^{1/2}\}. \quad (2c)$$

Here  $\theta_t$  is given by

$$\theta_t = \sin^{-1}\left(\frac{1}{n} \sin\theta_{inc}\right), \quad (2d)$$

and the Fresnel transmission coefficients  $\tau_x^A$ ,  $\tau_y^A$ , and  $\tau_z^A$  are, respectively, given by<sup>8</sup>

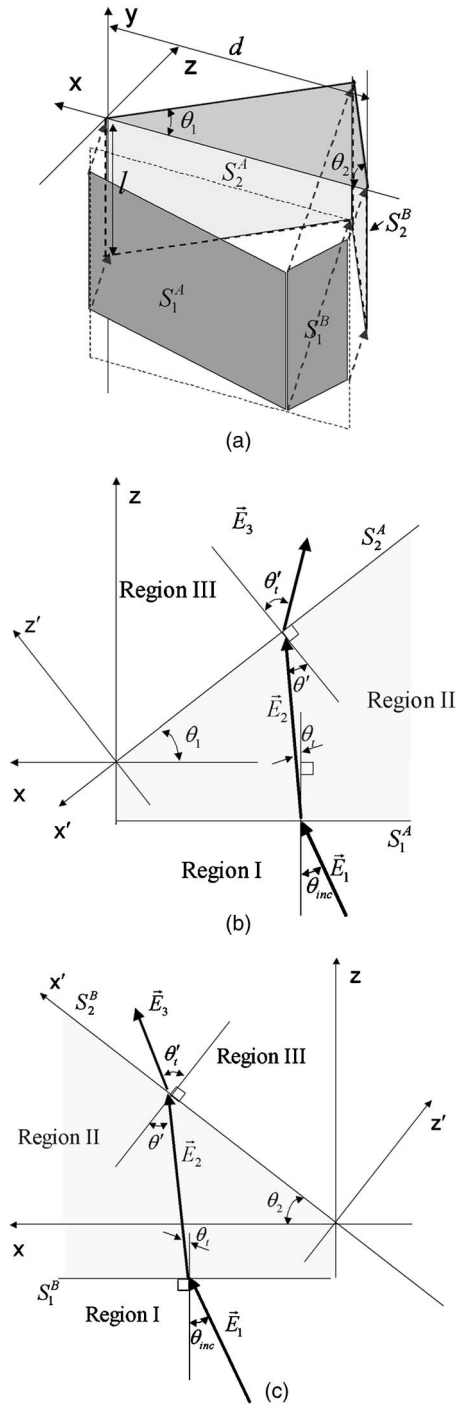


**Fig. 2** Incident plane wave is incident on the rear side of a prism sheet and propagates inside a unit prism along two separated paths,  $S_1^A \rightarrow S_2^A$  and  $S_1^B \rightarrow S_2^B$ : (a) 3-D view of two paths and 2-D views of (b) the path  $S_1^A \rightarrow S_2^A$  and (c) the path  $S_1^B \rightarrow S_2^B$ .

$$\begin{aligned} \tau_x^A &= \tau_x(\theta_{inc}, \phi, \psi, 1, n) \\ &= \frac{\tau_{TM} \cos \psi \cos \theta_i \cos \phi - \tau_{TE} \sin \psi \sin \phi}{\cos \psi \cos \theta_{inc} \cos \phi - \sin \psi \sin \phi}, \end{aligned} \quad (2e)$$

$$\begin{aligned} \tau_y^A &= \tau_y(\theta_{inc}, \phi, \psi, 1, n) \\ &= \frac{\tau_{TM} \cos \psi \cos \theta_i \sin \phi + \tau_{TE} \sin \psi \cos \phi}{\cos \psi \cos \theta_{inc} \sin \phi + \sin \psi \cos \phi}, \end{aligned} \quad (2f)$$

and

$$\tau_z^A = \tau_z(\theta_{inc}, \phi, \psi, 1, n) = \frac{\tau_{TM} \sin \theta_i}{\sin \theta}. \quad (2g)$$

As shown in Fig. 2(a), the refracted wave  $\vec{E}_2$  is divided into two portions. The first portion illuminates the facet  $S_2^A$  through the facet  $S_1^A$  precisely, as indicated in Fig. 2(b). Similarly, the second portion illuminates the facet  $S_2^B$  through the facet  $S_1^B$  precisely, as shown in Fig. 2(c). We consider the portion of the wave illuminating the facet  $S_1^A$  first. Rotating vectors on the coordinate system  $(x, y, z)$  by  $\theta_1$  around the  $y$  axis, we can obtain the representation of  $\vec{E}_2$  on the rotated coordinate  $(x', y', z')$  as follows:

$$\begin{aligned} \vec{E}_2 &= [(u_{2,x} \cos \theta_1 - u_{2,z} \sin \theta_1) \hat{x}' + u_{2,y} \hat{y}' + (u_{2,x} \sin \theta_1 \\ &\quad + u_{2,z} \cos \theta_1) \hat{z}'] \exp\{j[(k_{2,x} \cos \theta_1 - k_{2,z} \sin \theta_1) x' \\ &\quad + k_{2,y} y' + (k_{2,x} \sin \theta_1 + k_{2,z} \cos \theta_1) z']\} \\ &= (u'_{2,x} \hat{x}' + u'_{2,y} \hat{y}' + u'_{2,z} \hat{z}') \exp[j(k'_{2,x} x' + k'_{2,y} y' + k'_{2,z} z')]. \end{aligned} \quad (3)$$

Then,  $\vec{E}_2$  is incident on the facet  $S_2^A$  and refracted into region III. The refracted wave is denoted by  $\vec{E}_3$  which is represented by

$$\vec{E}_3 = (u'_{3,x} \hat{x}' + u'_{3,y} \hat{y}' + u'_{3,z} \hat{z}') \exp[j(k'_{3,x} x' + k'_{3,y} y' + k'_{3,z} z')], \quad (4a)$$

where  $(u'_{3,x}, u'_{3,y}, u'_{3,z})$  and  $(k'_{3,x}, k'_{3,y}, k'_{3,z})$  are, respectively, given by

$$(u'_{3,x}, u'_{3,y}, u'_{3,z}) = (\tau_x^{A'} u'_{2,x}, \tau_y^{A'} u'_{2,y}, \tau_z^{A'} u'_{2,z}), \quad (4b)$$

and

$$\begin{aligned} (k'_{3,x}, k'_{3,y}, k'_{3,z}) &= \{k'_{2,x}, k'_{2,y}, k_0 [1 - (n \sin \theta')^2]^{1/2}\} \\ &= (k'_{2,x}, k'_{2,y}, k_0 \cos \theta'). \end{aligned} \quad (4c)$$

Here,  $(\tau_x^{A'}, \tau_y^{A'}, \tau_z^{A'})$ ,  $(\cos \phi', \sin \phi')$ , and  $(\cos \psi', \sin \psi')$  are, respectively, defined as

$$\begin{aligned} \tau_x^{A'} &= \tau_x(\theta', \phi', \psi', n, 1) \\ &= \frac{\tau'_{TM} \cos \psi' \cos \theta'_i \cos \phi' - \tau'_{TE} \sin \psi' \sin \phi'}{\cos \psi' \cos \theta' \cos \phi' - \sin \psi' \sin \phi'}, \end{aligned} \quad (4d)$$

$$\begin{aligned} \tau_y^{A'} &= \tau_y(\theta', \phi', \psi', n, 1) \\ &= \frac{\tau'_{TM} \cos \psi' \cos \theta'_i \sin \phi' + \tau'_{TE} \sin \psi' \cos \phi'}{\cos \psi' \cos \theta' \sin \phi' + \sin \psi' \cos \phi'}, \end{aligned} \quad (4e)$$

$$\tau_z^{A'} = \tau_z(\theta', \phi', \psi', n, 1) = \frac{\tau'_{TM} \sin \theta'_i}{\sin \theta'}, \quad (4f)$$

$$(\cos \phi', \sin \phi') = \left\{ \begin{array}{l} \frac{k'_{2,x}}{[(k'_{2,x})^2 + (k'_{2,y})^2]^{1/2}}, \\ \frac{k'_{2,y}}{[(k'_{2,x})^2 + (k'_{2,y})^2]^{1/2}} \end{array} \right\}, \quad (4g)$$

and

$$(\cos \psi', \sin \psi') = \left[ \begin{array}{l} \frac{\cos \phi' u'_{2,x} + \sin \phi' u'_{2,y}}{(\cos^2 \theta' (u'^2_{2,x} + u'^2_{2,y} + u'^2_{2,z})^{1/2})} \\ - \frac{\sin \phi' u'_{2,x} + \cos \phi' u'_{2,y}}{(u'^2_{2,x} + u'^2_{2,y} + u'^2_{2,z})^{1/2}} \end{array} \right]. \quad (4h)$$

Here,  $\theta'$  and  $\theta'_i$  are, respectively, given by

$$\theta' = \cos^{-1} \left( \frac{k_{1,x} \sin \theta_1 + k_{1,z} \cos \theta_1}{k_0 n} \right) \quad (4i)$$

and

$$\theta'_i = \sin^{-1}(n \sin \theta'). \quad (4j)$$

The power is obtained by multiplying the intensity and the projected area illuminated by the optical wave. Figure 2(a) manifests the projected areas on the rear side and the front side of the prism sheet. To calculate the transmitted power, the intensity of the transmitted waves  $I_2^A$  and  $I_3^A$  through the facets  $S_1^A$  and  $S_2^A$ , and the areas of  $S_1^A$  and  $S_2^A$  are, respectively, obtained as

$$I_2^A = |\mathbf{E}_2|^2 = |u_{2,x}|^2 + |u_{2,y}|^2 + |u_{2,z}|^2 = |\tau_x^A u_{1,x}|^2 + |\tau_y^A u_{1,y}|^2 + |\tau_z^A u_{1,z}|^2, \quad (5)$$

$$I_3^A = |\mathbf{E}_3|^2 = |u'_{3,x}|^2 + |u'_{3,y}|^2 + |u'_{3,z}|^2 = |\tau_x^A|^2 |\tau_x^A u_{1,x} \cos \theta_1 - \tau_z^A u_{1,z} \sin \theta_1|^2 + |\tau_y^A|^2 |\tau_y^A u_{1,y}|^2 + |\tau_z^A|^2 |\tau_x^A u_{1,x} \sin \theta_1 + \tau_z^A u_{1,z} \cos \theta_1|^2, \quad (6)$$

$$d(S_1^A) = ld \left| \frac{\cos \theta_1 \sin \theta_2}{\sin(\theta_1 + \theta_2)} + \frac{\sin \theta_1 \sin \theta_2}{\sin(\theta_1 + \theta_2)} \left( \frac{k_{2,x}}{k_{2,z}} \right) \right|, \quad (7)$$

and

$$d(S_2^A) = \frac{ld \sin \theta_2}{\sin(\theta_1 + \theta_2)}, \quad (8)$$

where  $d(S_1^A)$  and  $d(S_2^A)$  denote the areas of the facets  $S_1^A$  and  $S_2^A$ , respectively. Two matters that require attention are, respectively, as follows:

1. If  $k'_{2,z}$  in Eq. (3) is nonpositive, i.e.,  $k'_{2,z} \leq 0$ , the facet  $S_2^A$  cannot be illuminated, which can be called the shadowing effect. In this case, the whole incident light goes along the path  $S_1^B \rightarrow S_2^B$ .
2. Although the light may illuminate the facet  $S_2^A$ , total internal reflection may occur at the boundary of the facet.

In both cases, the power transmitted through the facet  $S_2^A$  is

set to zero. These points are carefully taken into account in the case of considering the portion of the wave illuminating the facet  $S_1^B$ .

By the simple way of replacing  $\theta_1$  with  $-\theta_2$  and manipulating similar mathematics, the intensities of the transmitted wave  $I_2^B$  and  $I_3^B$  and the areas of  $S_1^B$  and  $S_2^B$  can be, respectively, obtained as

$$I_2^B = |\tau_x^B u_{1,x}|^2 + |\tau_y^B u_{1,y}|^2 + |\tau_z^B u_{1,z}|^2, \quad (9)$$

$$I_3^B = |\tau_x^B|^2 |\tau_x^B u_{1,x} \cos \theta_2 + \tau_z^B u_{1,z} \sin \theta_2|^2 + |\tau_y^B|^2 |\tau_y^B u_{1,y}|^2 + |\tau_z^B|^2 |-\tau_x^B u_{1,x} \sin \theta_2 + \tau_z^B u_{1,z} \cos \theta_2|^2, \quad (10)$$

$$d(S_1^B) = ld \left| \frac{\cos \theta_2 \sin \theta_1}{\sin(\theta_1 + \theta_2)} - \frac{\sin \theta_1 \sin \theta_2}{\sin(\theta_1 + \theta_2)} \left( \frac{k_{2,x}}{k_{2,z}} \right) \right|, \quad (11)$$

and

$$d(S_2^B) = \frac{ld \sin \theta_1}{\sin(\theta_1 + \theta_2)}. \quad (12)$$

Therefore, we can obtain the transmitted powers  $T_1^A$  and  $T_2^A$  through  $S_1^A$  and  $S_2^A$ , respectively, as

$$T_1^A = ldn \cos \theta_i \left| \frac{\cos \theta_1 \sin \theta_2}{\sin(\theta_1 + \theta_2)} + \frac{\sin \theta_1 \sin \theta_2}{\sin(\theta_1 + \theta_2)} \left( \frac{k_{2,x}}{k_{2,z}} \right) \right| I_2^A, \quad (13)$$

and

$$T_2^A = \frac{ld \sin \theta_2 \cos \theta'_i}{\sin(\theta_1 + \theta_2)} I_3^A, \quad (14)$$

where  $\theta'_i$  is given by Eq. (4j). In the same way, the transmitted powers through  $S_1^B$  and  $S_2^B$  are, respectively, obtained as

$$T_1^B = ldn \cos \theta_i \left| \frac{\cos \theta_2 \sin \theta_1}{\sin(\theta_1 + \theta_2)} - \frac{\sin \theta_1 \sin \theta_2}{\sin(\theta_1 + \theta_2)} \left( \frac{k_{2,x}}{k_{2,z}} \right) \right| I_2^B, \quad (15)$$

and

$$T_2^B = \cos \theta'_i S_2^B I_3^B = \frac{ld \sin \theta_1 \cos \theta'_i}{\sin(\theta_1 + \theta_2)} I_3^B, \quad (16)$$

where  $\theta'_i$  is obtained by substituting  $-\theta_2$  into  $\theta_1$  in Eqs. (4i) and (4j). The total energy incident on the unit cell of prism sheet is given by

$$(|u_{1,x}|^2 + |u_{1,y}|^2 + |u_{1,z}|^2)(S_1^A + S_1^B) \cos \theta_{\text{inc}} = E_0^2 ld \cos \theta_{\text{inc}}. \quad (17)$$

## 2.2 Oblique Incidence of a Plane Wave on the Front Side of Prism Sheets

The transmissivity of the prism sheet is analyzed when an incident plane wave propagates from the front side to the rear side of the prism sheet [see Fig. 1(b)]. Figure 3 shows

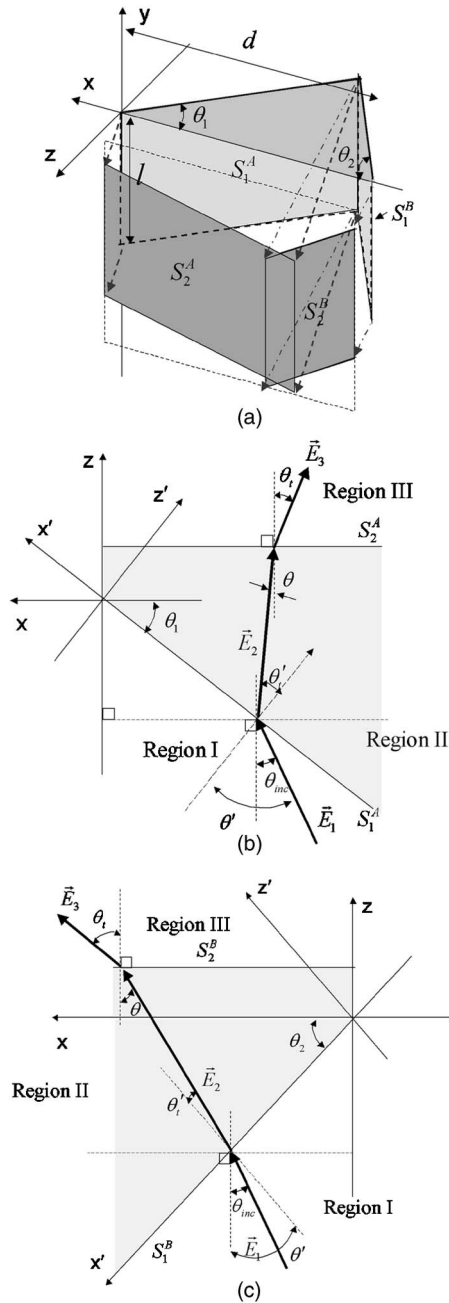


**Fig. 3** Incident plane wave is incident on the front side of a prism sheet and propagates inside a unit prism along two separated paths,  $S_1^A \rightarrow S_2^A$  and  $S_1^B \rightarrow S_2^B$ . (a) 3-D view of two paths and two-dimensional views of (b) the path  $S_1^A \rightarrow S_2^A$  and (c) the path  $S_1^B \rightarrow S_2^B$ .

traces of rays passing through facets of prism sheets. As in the previous section, we separately look into ray trace along two separated paths  $S_1^A \rightarrow S_2^A$  and  $S_1^B \rightarrow S_2^B$ , respectively, indicated in Fig. 3(a). The electric field in region I  $\mathbf{E}_1$  is given by Eq. (1a). As seen in Fig. 3(a), the incident wave  $\mathbf{E}_1$  is divided into two portions. The first portion illuminates the facet  $S_2^A$  through the area  $S_1^A$  precisely, as indicated in Fig. 3(b). Similarly, the second portion illuminates the facet  $S_2^B$  through the facet  $S_1^B$  precisely, as shown in Fig. 3(c). The portion of the wave incident on the facet  $S_1^A$  is considered at

first. Rotating vectors on the coordinate system  $(x, y, z)$  by  $\theta_1$  around the  $y$  axis, we obtain the representation of  $\mathbf{E}_1$  on the rotated coordinate  $(x', y', z')$  as

$$\mathbf{E}_1 = (u'_{1,x}\hat{x}' + u'_{1,y}\hat{y}' + u'_{1,z}\hat{z}') \exp[j(k'_{1,x}x' + k'_{1,y}y' + k'_{1,z}z')], \quad (18a)$$

where  $(u'_{1,x}, u'_{1,y}, u'_{1,z})$  and  $(k'_{1,x}, k'_{1,y}, k'_{1,z})$  are, respectively, given by

$$(u'_{1,x}, u'_{1,y}, u'_{1,z}) = (u_{1,x} \cos \theta_1 + u_{1,z} \sin \theta_1, u_{1,y}, -u_{1,x} \sin \theta_1 + u_{1,z} \cos \theta_1), \quad (18b)$$

and

$$(k'_{1,x}, k'_{1,y}, k'_{1,z}) = (k_{1,x} \cos \theta_1 + k_{1,z} \sin \theta_1, k_{1,y}, -k_{1,x} \sin \theta_1 + k_{1,z} \cos \theta_1). \quad (18c)$$

When  $\mathbf{E}_1$  meets the prism sheet,  $\mathbf{E}_1$  is refracted into region II. The refracted wave in region II  $\mathbf{E}_2$  is represented as

$$\mathbf{E}_2 = (u'_{2,x}\hat{x}' + u'_{2,y}\hat{y}' + u'_{2,z}\hat{z}') \exp[j(k'_{2,x}x' + k'_{2,y}y' + k'_{2,z}z')], \quad (19a)$$

where  $(u'_{2,x}, u'_{2,y}, u'_{2,z})$  and  $(k'_{2,x}, k'_{2,y}, k'_{2,z})$  are, respectively, defined as

$$(u'_{2,x}, u'_{2,y}, u'_{2,z}) = (\tau_x^{A'} u'_{1,x}, \tau_y^{A'} u'_{1,y}, \tau_z^{A'} u'_{1,z}), \quad (19b)$$

and

$$(k'_{2,x}, k'_{2,y}, k'_{2,z}) = \{k'_{1,x}, k'_{1,y}, k_0 n [1 - (\sin \theta' / n)^2]^{1/2}\}. \quad (19c)$$

Here,  $\theta'$ ,  $\theta'_t$ ,  $\tau_x^{A'}$ ,  $\tau_y^{A'}$ , and  $\tau_z^{A'}$  are, respectively, given by

$$\theta' = \cos^{-1} \left( \frac{-k_{1,x} \sin \theta_1 + k_{1,z} \cos \theta_1}{k_0 n} \right), \quad (19d)$$

$$\theta'_t = \sin^{-1} \left( \frac{1}{n} \sin \theta' \right), \quad (19e)$$

$$\begin{aligned} \tau_x^{A'} &= \tau_x(\theta', \phi', \psi', 1, n) \\ &= \frac{\tau'_{TM} \cos \psi' \cos \theta'_t \cos \phi' - \tau'_{TE} \sin \psi' \sin \phi'}{\cos \psi' \cos \theta' \cos \phi' - \sin \psi' \sin \phi'}, \end{aligned} \quad (19f)$$

$$\begin{aligned} \tau_y^{A'} &= \tau_y(\theta', \phi', \psi', 1, n) \\ &= \frac{\tau'_{TM} \cos \psi' \cos \theta'_t \sin \phi' + \tau'_{TE} \sin \psi' \cos \phi'}{\cos \psi' \cos \theta' \sin \phi' + \sin \psi' \cos \phi'}, \end{aligned} \quad (19g)$$

and

$$\tau_z^{A'} = \tau_z(\theta', \phi', \psi', 1, n) = \frac{\tau'_{TM} \sin \theta'_t}{\sin \theta'}, \quad (19h)$$

where  $(\cos \phi', \sin \phi')$  and  $(\cos \psi', \sin \psi')$  are, respectively, obtained as

$$(\cos \phi', \sin \phi') = \left\{ \frac{k'_{1,x}}{[(k'_{1,x})^2 + (k'_{1,y})^2]^{1/2}}, \frac{k'_{1,y}}{[(k'_{1,x})^2 + (k'_{1,y})^2]^{1/2}} \right\} \quad (19i)$$

and

$$(\cos \psi', \sin \psi') = \left[ \frac{\cos \phi' u'_{1,x} + \sin \phi' u'_{1,y}}{\cos \theta' (u'^2_{1,x} + u'^2_{1,y} + u'^2_{1,z})^{1/2}}, \frac{-\sin \phi' u'_{1,x} + \cos \phi' u'_{1,y}}{(u'^2_{1,x} + u'^2_{1,y} + u'^2_{1,z})^{1/2}} \right]. \quad (19j)$$

Next, we represent  $\mathbf{E}_2$  on the counter rotated coordinate  $(x, y, z)$  as follows

$$\begin{aligned} \mathbf{E}_2 = & [(u'_{2,x} \cos \theta_1 - u_{2,z} \sin \theta_1)\hat{x} + u'_{2,y}\hat{y} + (u'_{2,x} \sin \theta_1 \\ & + u'_{2,z} \cos \theta_1)\hat{z}] \exp[j(k'_{2,x} \cos \theta_1 - k'_{2,z} \sin \theta_1)x + k'_{2,y}y \\ & + (k'_{2,x} \sin \theta_1 + k'_{2,z} \cos \theta_1)z] \\ = & (u_{2,x}\hat{x} + u_{2,y}\hat{y} + u_{2,z}\hat{z}) \exp[j(k_{2,x}x + k_{2,y}y + k_{2,z}z)]. \quad (20) \end{aligned}$$

Then  $\mathbf{E}_2$  is incident on the facet  $S_2^A$  and refracted into region III. The refracted wave  $\mathbf{E}_3$  is represented as

$$\mathbf{E}_3 = (u_{3,x}\hat{x} + u_{3,y}\hat{y} + u_{3,z}\hat{z}) \exp[j(k_{3,x}x + k_{3,y}y + k_{3,z}z)], \quad (21a)$$

where  $(u_{3,x}, u_{3,y}, u_{3,z})$  and  $(k_{3,x}, k_{3,y}, k_{3,z})$  are, respectively, given by

$$(u_{3,x}, u_{3,y}, u_{3,z}) = (\tau_x^A u_{2,x}, \tau_y^A u_{2,y}, \tau_z^A u_{2,z}) \quad (21b)$$

and

$$(k_{3,x}, k_{3,y}, k_{3,z}) = \{k_{2,x}, k_{2,y}, k_0[1 - (n \sin \theta)^2]^{1/2}\}. \quad (21c)$$

Here,  $\tau_x^A, \tau_y^A, \tau_z^A, (\cos \theta, \sin \theta), (\cos \phi, \sin \phi), (\cos \psi, \sin \psi)$ , and  $\theta_t$  are, respectively, defined by

$$\begin{aligned} \tau_x^A = & \tau_x(\theta, \phi, \psi, n, 1) \\ = & \frac{\tau_{TM} \cos \psi \cos \theta_t \cos \phi - \tau_{TE} \sin \psi \sin \phi}{\cos \psi \cos \theta \cos \phi - \sin \psi \sin \phi}, \quad (21d) \end{aligned}$$

$$\begin{aligned} \tau_y^A = & \tau_y(\theta, \phi, \psi, n, 1) \\ = & \frac{\tau_{TM} \cos \psi \cos \theta_t \sin \phi + \tau_{TE} \sin \psi \cos \phi}{\cos \psi \cos \theta \sin \phi + \sin \psi \cos \phi}, \quad (21e) \end{aligned}$$

$$\tau_z^A = \tau_z(\theta, \phi, \psi, 1, n) = \frac{\tau_{TM} \sin \theta_t}{\sin \theta}, \quad (21f)$$

$$(\cos \theta, \sin \theta) = \left\{ \frac{k_{1,z}}{k_0 n}, \left[ \left( \frac{k_{1,x}}{k_0 n} \right)^2 + \left( \frac{k_{1,y}}{k_0 n} \right)^2 \right]^{1/2} \right\}, \quad (21g)$$

$$(\cos \phi, \sin \phi) = \left\{ \frac{k_{1,x}}{[(k_{1,x})^2 + (k_{1,y})^2]^{1/2}}, \frac{k_{1,y}}{[(k_{1,x})^2 + (k_{1,y})^2]^{1/2}} \right\}, \quad (21h)$$

$$(\cos \psi, \sin \psi) = \left[ \frac{\cos \phi u_{1,x} + \sin \phi u_{1,y}}{\cos \theta (u_{1,x}^2 + u_{1,y}^2 + u_{1,z}^2)^{1/2}}, \frac{-\sin \phi u_{1,x} + \cos \phi u_{1,y}}{(u_{1,x}^2 + u_{1,y}^2 + u_{1,z}^2)^{1/2}} \right], \quad (21i)$$

and

$$\theta_t = \sin^{-1}(n \sin \theta). \quad (21j)$$

The powers transmitted through the facets  $S_1^A$  and  $S_2^A$  are respectively calculated by multiplying the intensity and the projected area illuminated by the optical wave. Figure 3(a) manifests the projected areas on the rear side and the front side of the prism sheet. To calculate the transmitted power, the intensities of the transmitted waves  $I_2^A$  and  $I_3^A$  through the facets  $S_1^A$  and  $S_2^A$ , and the areas of  $S_1^A$  and  $S_2^A$  are obtained as

$$\begin{aligned} I_2^A = & |\mathbf{E}_2|^2 = |u'_{2,x}|^2 + |u'_{2,y}|^2 + |u'_{2,z}|^2 \\ = & |\tau_x^A (u_{1,x} \cos \theta_1 + u_{1,z} \sin \theta_1)|^2 \\ & + |\tau_y^A u'_{1,y}|^2 + |\tau_y^A (-u_{1,x} \sin \theta_1 + u_{1,z} \cos \theta_1)|^2, \quad (22) \end{aligned}$$

$$\begin{aligned} I_3^A = & |\mathbf{E}_3|^2 = |u_{3,x}|^2 + |u_{3,y}|^2 + |u_{3,z}|^2 \\ = & |\tau_x^A|^2 [\tau_x^A (u_{1,x} \cos \theta_1 + u_{1,z} \sin \theta_1) \cos \theta_1 \\ & - \tau_z^A (-u_{1,x} \sin \theta_1 + u_{1,z} \cos \theta_1) \sin \theta_1]^2 + |\tau_y^A|^2 (\tau_y^A u_{1,y})^2 \\ & + |\tau_z^A|^2 [\tau_x^A (u_{1,x} \cos \theta_1 + u_{1,z} \sin \theta_1) \sin \theta_1 \\ & + \tau_z^A (-u_{1,x} \sin \theta_1 + u_{1,z} \cos \theta_1) \cos \theta_1]^2, \quad (23) \end{aligned}$$

$$d(S_1^A) = \frac{ld \sin \theta_2}{\sin(\theta_1 + \theta_2)}, \quad (24)$$

and

$$d(S_2^A) = ld \left| \frac{\cos \theta_1 \sin \theta_2}{\sin(\theta_1 + \theta_2)} - \frac{\sin \theta_1 \sin \theta_2}{\sin(\theta_1 + \theta_2)} \left( \frac{k_{2,x}}{k_{2,z}} \right) \right|. \quad (25)$$

As in the previous section, two matters that require attention are, respectively, as follows:

1. If  $k'_{1,z}$  in Eq. (3) is nonpositive, i.e.,  $k'_{1,z} \leq 0$ , facet  $S_2^A$  cannot be illuminated, which can be called the shadowing effect. In this case, the whole incident light goes along the path  $S_1^B \rightarrow S_2^B$ .
2. Although the light may illuminate facet  $S_2^A$ , total internal reflection may occur at the boundary of the facet.

In both cases, the power transmitted through the facet  $S_2^A$  is set to zero. This point is carefully taken into account in the case of considering the portion of the wave illuminating the facet  $S_1^B$ .

By replacing  $\theta_1$  with  $-\theta_2$  in the preceding equations, the intensities of the transmitted wave  $I_2^B$  and  $I_3^B$  and the areas of the facets  $S_1^B$  and  $S_2^B$  are, respectively, obtained as

$$I_2^B = |\tau_x^{B'}(u_{1,x} \cos \theta_2 - u_{1,z} \sin \theta_2)|^2 + |\tau_y^{B'} u_{1,y}'|^2 + |\tau_z^{B'}(u_{1,x} \sin \theta_2 + u_{1,z} \cos \theta_2)|^2, \quad (26)$$

$$I_3^B = |\tau_x^B|^2 [\tau_x^{B'}(u_{1,x} \cos \theta_2 - u_{1,z} \sin \theta_2) \cos \theta_1 + \tau_z^{B'}(u_{1,x} \sin \theta_2 + u_{1,z} \cos \theta_2) \sin \theta_2]^2 + |\tau_y^B|^2 (\tau_y^{B'} u_{1,y}')^2 + |\tau_z^B|^2 [-\tau_x^{B'}(u_{1,x} \cos \theta_2 - u_{1,z} \sin \theta_2) \sin \theta_2 + \tau_z^{B'}(u_{1,x} \sin \theta_2 + u_{1,z} \cos \theta_2) \cos \theta_2]^2, \quad (27)$$

$$d(S_1^B) = \frac{ld \sin \theta_1}{\sin(\theta_1 + \theta_2)}, \quad (28)$$

and

$$d(S_2^B) = ld \left| \frac{\cos \theta_2 \sin \theta_1}{\sin(\theta_1 + \theta_2)} + \frac{\sin \theta_1 \sin \theta_2}{\sin(\theta_1 + \theta_2)} \left( \frac{k_{2,x}}{k_{2,z}} \right) \right|. \quad (29)$$

Here, we can obtain the transmitted powers  $T_1^A$  and  $T_2^A$  through  $S_1^A$  and  $S_2^A$ , respectively, as

$$T_1^A = \frac{ld \sin \theta_2 \cos \theta_1'}{\sin(\theta_1 + \theta_2)} I_3^A, \quad (30)$$

and

$$T_2^A = ld \cos \theta_1' \left| \frac{\cos \theta_1 \sin \theta_2}{\sin(\theta_1 + \theta_2)} - \frac{\sin \theta_1 \sin \theta_2}{\sin(\theta_1 + \theta_2)} \left( \frac{k_{2,x}}{k_{2,z}} \right) \right| I_3^A, \quad (31)$$

where  $\theta_1'$  are given by Eq. (19e). The transmitted powers through  $S_1^B$  and  $S_2^B$  are, respectively, obtained as

$$T_1^B = \frac{ld \sin \theta_1 \cos \theta_1'}{\sin(\theta_1 + \theta_2)} I_3^B, \quad (32)$$

and

$$T_2^B = ld \cos \theta_1' \left| \frac{\cos \theta_2 \sin \theta_1}{\sin(\theta_1 + \theta_2)} + \frac{\sin \theta_1 \sin \theta_2}{\sin(\theta_1 + \theta_2)} \left( \frac{k_{2,x}}{k_{2,z}} \right) \right| I_3^B, \quad (33)$$

where  $\theta_1'$  are obtained by substituting  $-\theta_2$  into  $\theta_1$  in Eqs. (19d) and (19e). The total energy incident on the unit cell of prism sheet is the same as the case of the incidence on the rear side, as indicated in Eq. (17).

### 2.3 Optical Transmission Characteristics of a Single Prism Sheet

Mathematically, the calculation described in this paper is the definite representation of the conventional ray-tracing algorithm. Note, however, that the main point of the paper is the analytic calculation of the first-order trace of a local plane wave, which is a dense ray bundle with the same propagation direction. This approach reduces the computation time greatly by considering many rays with the same propagation direction at once.

In this section, using the developed analysis method, the optical transmission characteristics of a prism sheet are investigated. Using Eqs. (17), (31), and (33), the partial transmission coefficient distributions,  $\text{Tr}_A(\theta_{\text{inc}}, \phi)$ ,  $\text{Tr}_B(\theta_{\text{inc}}, \phi)$ ,

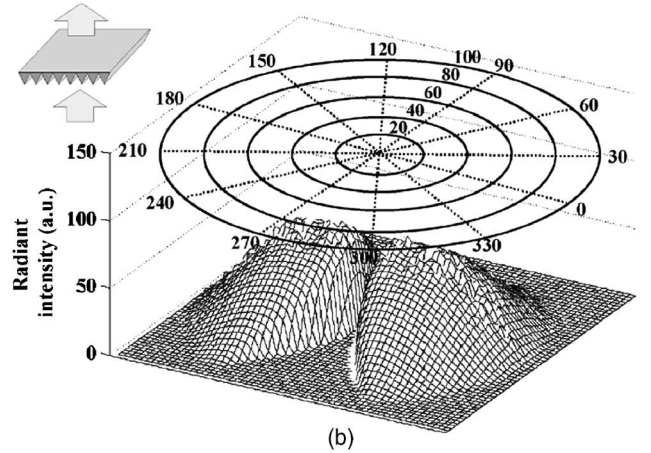
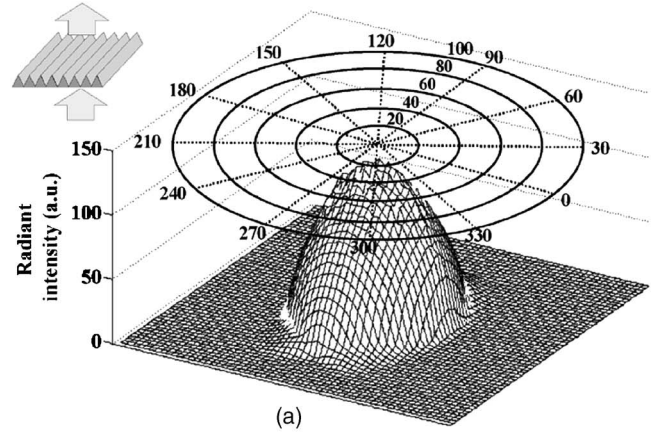


**Fig. 4** (a) Radiant intensity profile of the case of incidence on (a) the rear side of the prism sheet and (b) the front side of the prism sheet.

and the total transmission coefficient distribution  $\text{Tr}(\theta_{\text{inc}}, \phi)$  for incident plane wave with incidence angle of  $\theta_{\text{inc}}$  and azimuthal angle of  $\phi$  are, respectively, defined as

$$\text{Tr}_A(\theta_{\text{inc}}, \phi) = \frac{\langle T_2^A \rangle_\psi}{ldE_0^2}, \quad (34a)$$

$$\text{Tr}_B(\theta_{\text{inc}}, \phi) = \frac{\langle T_2^B \rangle_\psi}{ldE_0^2}, \quad (34b)$$

and

$$\text{Tr}(\theta_{\text{inc}}, \phi) = \frac{\langle T_2^A + T_2^B \rangle_\psi}{ldE_0^2}, \quad (34c)$$

where it is noted that the power is viewed as an average for the polarization of light. The total transmission coefficient means the ratio of the power transmitted through the prism sheet to the power of the incident plane wave having unit intensity and illuminating unit area, while the partial transmission coefficient means the ratio of the power transmitted through the facets  $S_2^A$  or  $S_2^B$  to the incident power. We can also find the functional relations of the directions of the transmitted waves  $(\theta_A, \phi_A)$  and  $(\theta_B, \phi_B)$  to the direction of

the incident wave  $(\theta_{inc}, \phi)$  from Eqs. (4c) and (21c), respectively. Let these relations be represented as the following transforms  $f_A$  and  $f_B$ :

$$(\theta_B, \phi_B) \xleftarrow{f_B} (\theta_{inc}, \phi) \xrightarrow{f_A} (\theta_A, \phi_A). \quad (35)$$

Now, we can estimate the transmission characteristics of prism sheet for an incident light with arbitrary radiant intensity profile. If the radiant intensity profile of the incident light  $R_i(\theta_{inc}, \phi)$  is given as a function of  $(\theta_{inc}, \phi)$ , the inner products of two partial transmission coefficient distributions of the prism sheet  $\text{Tr}_A(\theta_{inc}, \phi)$  and  $\text{Tr}_B(\theta_{inc}, \phi)$ , and the radiant intensity profile  $R_i(\theta_{inc}, \phi)$  may translate into the partial radiant intensity profiles of the transmitted light  $R_{tA}(\theta_A, \phi_A)$  and  $R_{tB}(\theta_B, \phi_B)$ , respectively. That is, the following relations hold

$$R_{tA}(\theta_A, \phi_A) = \text{Tr}_A(\theta_{inc}, \phi) \cdot R_i(\theta_{inc}, \phi), \quad (36a)$$

and

$$R_{tB}(\theta_B, \phi_B) = \text{Tr}_B(\theta_{inc}, \phi) \cdot R_i(\theta_{inc}, \phi) \quad (36b)$$

where the inner product operator  $\cdot$  means

$$R_{t\sigma}(\theta_\sigma, \phi_\sigma) = \text{Tr}_\sigma(\theta_{inc}, \phi) R_i(\theta_{inc}, \phi) \quad (36c)$$

with  $f_\sigma$  in Eq. (35), ( $\sigma=A$  and  $B$ ). Then, we can also define the total radiant intensity profile or, simply, radiant intensity  $R_t$  as

$$R_t = R_{tA} + R_{tB}. \quad (36d)$$

The transmissivity of prism sheet  $T_s$  is defined as

$$T_s = \frac{\int_0^{2\pi} \int_0^{\pi/2} [\text{Tr}_A(\theta_{inc}, \phi) R_i(\theta_{inc}, \phi) + \text{Tr}_B(\theta_{inc}, \phi) R_i(\theta_{inc}, \phi)] \sin \theta_{inc} d\theta_{inc} d\phi}{\int_0^{2\pi} \int_0^{\pi/2} R_i(\theta_{inc}, \phi) \sin \theta_{inc} d\theta_{inc} d\phi}. \quad (37)$$

The transmissivity means the ratio of the total power transmitted through the prism sheet to the power of the incident light.

In general, a prism sheet is equipped in a backlight module. The backlight module is designed to recycle the portion of the incident light reflected by the prism sheet. The reflected light is reshaped by diffuser and reflection film and recycled in the backlight module to be incident on the prism sheet. If the diffuser is ideal, it is plausible to assume that both the initial incident light and the recycled incident light have Lambertian radiant intensity profile.

A Lambertian light is composed of incoherent plane waves with the radiant intensity profile,  $R_{\text{Lam}}(\theta_{inc}, \phi)$ , given by

$$R_{\text{Lam}}(\theta_{inc}, \phi) = I_0 \cos \theta_{inc}. \quad (38)$$

Thus, the radiant intensity profile of the transmitted light  $R_t$  is obtained by substituting Eq. (38) into Eqs. (36a)–(36d).

Using the Lambertian light as the incident light, we can obtain output radiant intensity profiles, as shown in Fig. 4. In this paper, it is assumed that since the recycled incident light is also a Lambertian light, the radiant intensity profile of the transmitted light is invariant by the recycling. Thus, we consider only the responses of the initial light incidence in the simulations. In the simulation, the refractive index  $n$  of the prism sheet is 1.5, and the first and second base angles of a unit prism  $\theta_1$  and  $\theta_2$  are equally 45 deg. In addition,  $l=1$  and  $d=1$  are settled without loss of generality (see Figs. 2 and 3). Radiant intensity profiles of the cases of incidence on the rear side and the front side represented on the polar coordinate of incidence angle and azimuthal angle

are shown in Figs. 4(a) and 4(b), respectively, where degrees are used for angle dimension instead of radians.

In the case of incidence on the rear side, prism sheet condenses incident Lambertian light as shown in Fig. 4(a), while in the case of incidence on the front side prism sheet divides radiant intensity profile to two separated regions. In the case of the incidence on the rear side, the rays with small incidence angles, i.e., those with near normal direction, are totally reflected by the two hypotenuses of the prism sheet, but the rays with almost normal directions to the hypotenuses can be refracted into the region III. On the other hand, in the case of the incidence on the front side, the rays with small incidence angles does not experience total internal reflections, but the directions of the transmitted rays in the region III are gathered about the region indicated in Fig. 4(b). As stated in Eq. (37), the transmissivity is just simple summation of all power projected on the virtual hemisphere around the prism sheet contributed by a plane wave component. For the Lambertian light, the transmissivities are respectively obtained as 42.2 and 77.8% for the cases of incidence on the rear and the front sides.

The structure of a single prism sheet is determined by three design parameters, refractive index and two base angles. Dependencies of transmissivity on refractive index and two base angles are inspected. In Fig. 5, variation of transmissivity with changes in two base angles for a fixed refractive index is presented. Figure 5 shows the transmissivity decreases gradually as the base angle increases for both cases of incidence on the rear side and front side of prism sheet. Comparing Figs. 5(a) and 5(b), we can see that

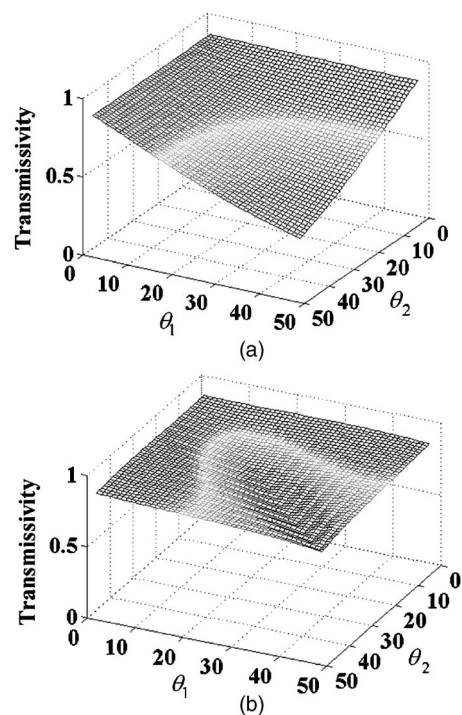


**Fig. 5** Variations of transmissivity with changes in the base angles  $\theta_1$  and  $\theta_2$  (a) in the case of incidence on (a) the rear side of prism sheet and (b) the front side of prism sheet.

the variation of the transmissivity in case of incidence on the rear side is more sensitive to the change in base angles. For any pair of  $(\theta_1, \theta_2)$ , transmissivity of the case of the incidence on the rear side is higher than that of the case of the incidence on the front side. Figure 6 shows variation of transmissivity with changes in refractive index and common base angle for isosceles prism sheet. It is shown that for a given base angle, the transmissivity decreases with the increase in refractive index. In both cases of incidence on the rear side and front side, it is recognized that when the refractive index is higher, the transmissivity decreases faster when lowering the base angle.

When the conventional ray tracing means that many rays with energy weight factors meet a facet, then the power transmitted through the facet is calculated by summing up all transmitted ray energy. Note, however, that in our approach, no individual ray tracing is used, but the local plane waves are traced. Conceptually, the numbers of rays with the same propagation direction meet the area of the facets in our method. The derived analytic formulas are directly used to calculate radiant intensity profile of the transmitted light and transmissivity, which accounts for the decrease in computation time.

### 3 Generalized Analysis of the Transmissivity of the Prism Sheet Layer

In this section, the optical transmission characteristics of prism sheet layer for Lambertian light are investigated. A simple method to calculate the transmission characteristic of prism sheet layer is proposed based on the theory established in previous sections. In Sec. 2, we made the functional relation of output radiant intensity profile to input

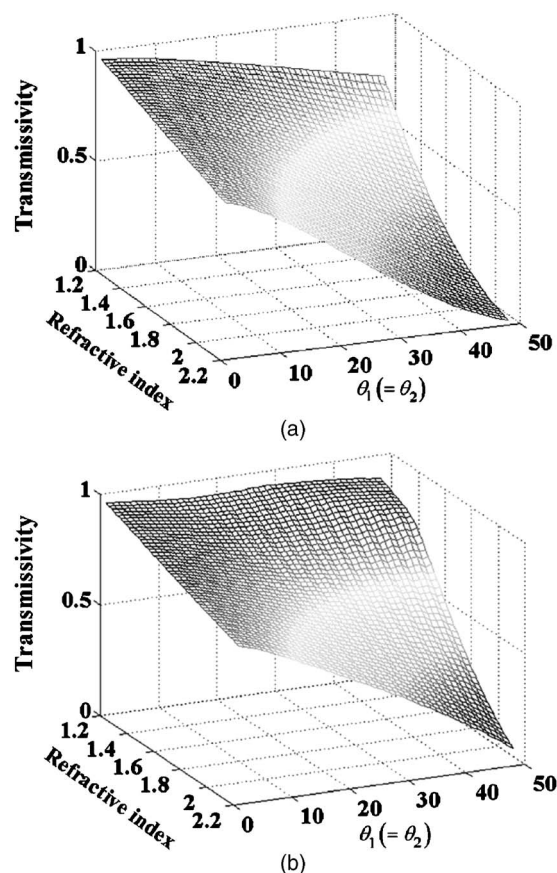


**Fig. 6** Variations of transmissivity with changes in the refractive index and the common base angles  $\theta_1(=\theta_2)$  of isosceles prism sheet in the case of incidence on (a) the rear side of prism sheet and (b) the front side of prism sheet.

radiant intensity profile by building up two partial transmission coefficient distributions. The main idea of prism sheet layer analysis is that the output radiant intensity profile obtained through the first prism sheet is used as the input radiant intensity profile to the second prism sheet.

The output radiant intensity profiles of the cases of incidence on the rear side and the front side of a single prism sheet are presented in Figs. 4(a) and 4(b), respectively. In the simulation, the refractive index  $n$  is 1.5, and the first and second base angles of a unit prism  $\theta_1$  and  $\theta_2$  of all prism sheets are equally set to 45 deg. We can deal with layer structures composed of many prism sheets similarly by iterative execution of the described procedure.

Figure 7 shows radiant intensity profiles obtained through basic combinatorial arrangements of the layer of two same prism sheets with input as Lambertian light. It is shown that each arrangement generates its own specific radiant intensity profile. The layer of two prism sheets is determined by six structure parameters. Without changing the basic arrangement, by modification of some design parameters, the radiant intensity profiles are considerably reformed or distorted within the extent of conserving the fundamental patterns presented in Fig. 7. In the case of Fig. 7(a), the light incident on the front side of the first prism sheet is divided into two portions. Successively, each portion is refracted by the second prism sheet to form the four

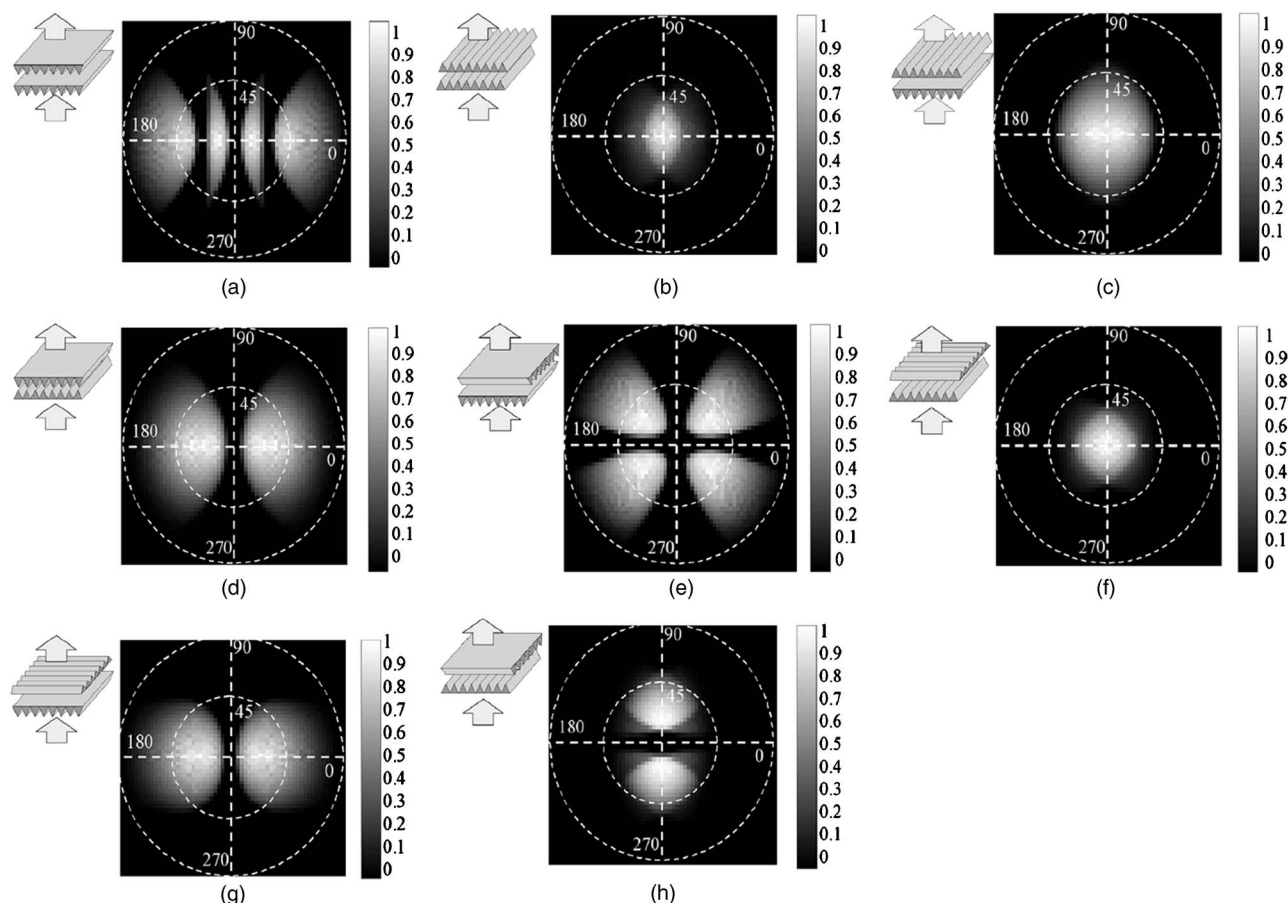


**Fig. 7** Radiant intensity profiles of various combinational arrangements of two same-type prism sheets.

divided regions in the output radiant intensity profile. By a similar analogy, all patterns illustrated in Figs. 7 can be simply interpreted.

Practically, for backlight modules, the arrangement indicated in Fig. 7(f), i.e., 3M's BEF structure, is desirable since the radiant intensity profile is localized near the center, comparatively.

However, it is desirable to make an effort to optimize the stack of prism sheets further and contemplate appropriate applications for other arrangements. Since the computation time for obtaining the radiant intensity profile through the proposed method is much shorter than that for the conventional ray-tracing method, it is feasible to design the optimal structure of a stack of prism sheets by using matured optimization techniques such as a genetic algorithm and simulated annealing.

#### 4 Conclusion

In this paper, an analytic method for analyzing optical transmission characteristics of prism sheets (BEF structure) was presented. The partial transmission coefficient distribution of a prism sheet was respectively defined for the cases of incidence on the rear side and the front side of prism sheet. The incident light to a prism sheet was characterized by its own radiant intensity profile. It was shown that the output radiant intensity profile is the inner product of the

newly defined total transmission coefficient distribution of the prism sheet and the input radiant intensity profile. In addition, a systematic method for analyzing a prism sheet layer was described based on the developed analysis method. Although the prism sheet analyzed in this paper was selected as the simplest structure, i.e., BEF, the developed analysis methodology can be extended to more general and various structures of prism sheets with many facets.

The proposed method does not take multiple reflections inside prism sheet and multiple scattering between adjacent unit prisms into account. An additional simplification of the proposed method is that the region with transmittance coefficient of zero that is totally reflected inside the prism sheet is not taken into account in the analysis. In the case of incidence on the front side, rays with large incidence angle can be reflected to the front side by the total internal reflection. However, if the incident light has low energy in the large incidence angle, as for Lambertian light, our ignorance of the total internal reflection does not induce a large difference in the transmissivity from the conventional ray-tracing algorithm. We think that an analytic calculation considering the effect of the total internal reflection is feasible, but requires further investigation.

In conclusion, the advantage of greatly reducing computation time over conventional time-consuming ray-tracing

methods may make the proposed method considerably useful for intuitive understanding of the optical characteristics of a stack of prism sheets and designing optimal prism sheet structures. It is desirable that the developed fast analytic method be used for design work, and the precise ray tracing software is employed to simulate the tuning of the designed structures.

### References

1. R. C. Allen, L. W. Carlson, A. J. Ouder Kirk, F. M. Weber, A. L. Kotz, T. J. Nevitt, C. A. Stover, and B. Majumdar, "Brightness enhancement film," U.S. Patent No. 6111696 (2000).
2. R. C. Allen, L. W. Carlson, A. J. Ouder Kirk, F. M. Weber, A. L. Kotz, T. J. Nevitt, C. A. Stover, and B. Majumdar, "Brightness enhancement film," U.S. Patent No. 6760157 (2004).
3. M. B. O'Neill and J. S. Cobb, "Brightness enhancement film with soft cutoff," U.S. Patent No. 5917664 (1999).
4. M. B. O'Neill and D. L. Wortman, "Luminance control film," U.S. Patent No. 6091547 (2000).
5. M. E. Gardiner, S. E. Cobb, K. A. Epstein, and W. D. Kretman, "Optical film with variable angle prisms," U.S. Patent No. 6707611 (2004).
6. M. Born and E. Wolf, *Principles of Optics*, 7th ed., Cambridge University Press, New York (1999).
7. L. Mandel and E. Wolf, *Optical Coherence and Quantum Optics*, Cambridge University Press, New York (1995).
8. H. Kim and B. Lee, "Calculation of the transmittance function of a multilevel diffractive optical element considering multiple internal reflections," *Opt. Eng.* **43**, 2671–2682 (2004).



**Hwi Kim** received his BS and MS degrees in 2001 and 2003, respectively, from the School of Electrical Engineering, Seoul National University, Korea, where he is currently a PhD candidate. His primary research interests are diffractive optics and photonic crystals.



**Yong Jun Lim** received his BS degree from the School of Electrical Engineering, Pusan National University, Korea, in 2004, and he is currently studying for his MS degree in the School of Electrical Engineering, Seoul National University. His primary research interests are hologram applications and surface plasmons.



**Byungchoon Yang** received his BS, MS, and PhD degrees from the School of Electrical Engineering from Seoul National University, Korea, in 1995, 1997, and 2002, respectively. He is currently with the research staff of Samsung Electronics Co. When the idea for this paper was initiated, he was with the Seoul National University. His primary research interests are LCD displays and holography.



**Kyongsik Choi** received his BS and MS degrees in electrical and electronic engineering from Chungbuk National University, Korea, in 1999 and 2001, respectively, and he is currently pursuing his PhD degree in the School of Electrical Engineering, Seoul National University. During 2000 and 2001 he was with the Samsung Advanced Institute of Technology. His primary research interests are bio- and nanophotonics, autostereoscopic 3-D display, diffractive optics, and optical information processing.



**Byoungho Lee** received his BS and MS degrees in electronics engineering in 1987 and 1989, respectively, from Seoul National University, Korea, and his PhD degree in electrical engineering and computer science in 1993 from the University of California at Berkeley. In 1994 he joined the faculty of the School of Electrical Engineering, Seoul National University, where he is now a professor. He became a fellow of the SPIE in 2002 and of the OSA in 2005. He is a senior member of the IEEE. He has served as a committee member for various international conferences. He has authored or coauthored more than 145 papers in international journals and more than 220 international conference papers. In 1999, his laboratory was honored as a National Research Laboratory by the Ministry of Science and Technology of Korea. In 2002 he received the Presidential Young Scientist Award of Korea. His research fields are hologram applications, 3-D displays, and optical fiber gratings.